Available online at www.sciencedirect.com
ScienceDirect
Trans. Nonferrous Met. Soc. China 22(2012) 1810−1816
Transactions of Nonferrous Metals Society of China
www.tnmsc.cn

Deformation defects and electron irradiation effect in nanostructured Al−Mg alloy processed by severe plastic deformation

LIU Man-ping[1,2], SUN Shao-chun[1], Hans J. ROVEN[2],
YU Ying-da[2], ZHANG Zhen[1], Maxim MURASHKIN[3], Ruslan Z. VALIEV[3]

1. School of Materials Science and Engineering, Jiangsu University, Zhenjiang 212013, China;
2. Department of Materials Science and Engineering,
Norwegian University of Science and Technology (NTNU), NO-7491, Trondheim, Norway;
3. Institute of Physics of Advanced Materials, Ufa State Aviation Technical University, Ufa 450000, Russia

Received 10 November 2011; accepted 18 July 2012

Abstract: In order to explore the exact nature of deformation defects previously observed in nanostructured Al−Mg alloys subjected to severe plastic deformation, a more thorough examination of the radiation effect on the formation of the planar defects in the high pressure torsion (HPT) alloys was conducted using high-resolution transmission electron microscopy (HRTEM). The results show that high density defects in the HRTEM images disappear completely when these images are exposed under the electron beam for some duration of time. At the same time, lattice defects are never observed within no-defect areas even when the beam-exposure increases to the degree that holes appear in the areas. Therefore, it is confirmed that the planar defects observed in the HPT alloys mainly result from the significant plastic deformation and are not due to the radiation effect during HRTEM observation.

Key words: Al−Mg alloy; severe plastic deformation; high pressure torsion; electron irradiation; deformation defects; transmission electron microscopy

1 Introduction

It is well established that bulk nanostructured materials (BNM) can be produced successfully via microstructural refinement using severe plastic deformation (SPD), i.e. heavy straining under high imposed pressure [1−6]. SPD processing is an attractive procedure for many advanced applications, as it allows enhancing significant properties of commonly used metals and alloys [2−4]. High pressure torsion (HPT) is one of the most promising SPD techniques because it has the potential to produce nanostructures with grain sizes of less than 100 nm [5,6]. Although outstanding progress has been made in this area in recent years, genesis of the structural features in SPD-processed metals is not yet fully understood [6−12]. In our previous work, deformation defects such as full and partial dislocations, dipoles, microtwins and stacking faults (SFs) have been frequently observed using transmission electron microscopy (TEM) and high-resolution TEM (HRTEM) in nanostructured Al−Mg alloys subjected to HPT [13−19]. However, some reports argue that such lattice defects along the {111} planes in Al and Al based alloys often form (and may disappear) due to the irradiation effect during HRTEM observation [20−28]. In order to explore the exact nature of these defects, a more thorough examination of the radiation effect on the formation of the planar defects in the HPT alloy is conducted in this study.

2 Experimental

A commercial AA5182 Al−Mg alloy (Al−4.1Mg−0.35Mn−0.13Si−0.32Fe, mass fraction, %) received in the as-cast and homogenized conditions was subjected to HPT to 5 turns at a rotation speed of 1 r/min under a pressure of 6 GPa at room temperature. The calculated

Foundation item: Project (50971087) supported by the National Natural Science Foundation of China; Project (BK2012715) supported by the Basic Research Program (Natural Science Foundation) of Jiangsu Province, China; Project (10371800) supported by the Research Council of Norway under the NEW Light (NEWLIGHT) Metals of the Strategic Area (SA) Materials; Project (11JDG070) supported by the Senior Talent Research Foundation of Jiangsu University, China
Corresponding author: LIU Man-ping; Tel: +86-511-88780192; E-mail: manping-liu@263.net; manpingliu@ujs.edu.cn
DOI: 10.1016/S1003-6326(11)61391-5

equivalent strain at the outer edge of the HPT samples is about 906 [2]. The dimensions of the deformed HPT samples were *d*20 mm×0.2 mm. Small disks with diameters of 3 mm were punched from the outer edge of these HPT samples. Thin TEM foils were prepared from the small disks by means of disc grinding, dimpling and finally ion polishing with Ar^+ at an accelerating voltage of 3 kV. The structural characterization was conducted by both JEM−2010 TEM and JEOL 2010F TEM operated at 200 kV.

3 Results and discussion

3.1 General microstructure

Figure 1(a) shows the general deformed microstructure observed in the AA5182 aluminum alloy together with selected area diffraction (SAD) pattern taken from 2.54 μm diameter region. The microstructure exhibits grain sizes in the 10–130 nm range and has a very small average grain size of about 55 nm. The grain size distribution is not uniform and grains with different sizes coexist. Dislocation cell structures and subgrains are frequently found inside some larger grains. The misorientation across these cell boundaries increases with further plastic straining, and eventually becomes large enough to transform through low angle grain boundaries (GBs) to high angle GBs [6]. In addition, some GBs in these larger grains are often curved and poorly defined or have a strong spreading of thickness extinction contours (Fig. 1(b)), indicating a high level of internal stresses and elastic distortions in the crystal lattice due to the presence of a local high dislocation density at the boundaries. All of these features suggest that these grains are in a nonequilibrium state with nonequilibrium GBs [6,13].

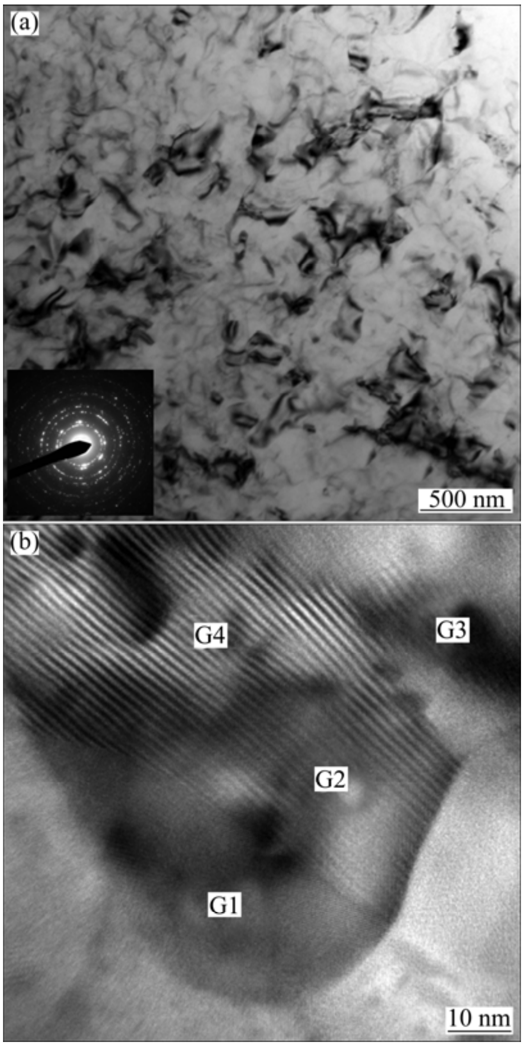

Fig. 1 TEM micrographs of HPT Al−Mg alloy: (a) Bright-field image with SAD pattern inset; (b) Typical grain with nonequilibrium GBs

3.2 Deformation defects

It is confirmed in our previous works that a high density of planar defects is often detected within smaller grains and subgrains with sizes of 20−50 nm [8,19]. The density varies from 10^{16} to 10^{18} m^{-2}. Some of the planar defects are confirmed by HRTEM to be deformation twins and SFs. Figure 2(a) shows another typical HRTEM image of these defects taken from the subgrain G1 in Fig. 1(b). The width of the subgrain is about 30 nm. The planar defects are indicated by white arrows. It is clearly evident that the planar defects have a habit plane of (111), as the white solid line indicated in Fig. 2(a). The multiple twins and SFs are highlighted in the Fourier-filtered image in Fig. 2(b). These twins are referred to as microtwins or nano-twins since the thickness of the twins spans only 1−4 atomic layers (0.2−1 nm) [19]. Such microtwins and SFs are believed to be formed behind the moving partial dislocations which are emitted from the sub-boundary. The microtwins and SFs are likely to heterogeneously nucleate at the sub-boundary and grow larger via the emission of Shockley partial dislocations from the sub-boundary [10]. Therefore, it is reasonable to conclude that the microtwins and SFs observed in Fig. 2 are formed through the heterogeneous mechanism.

Analogous to our previous works on HPT Al−Mg alloys [8,13], a high density of planar defects including SFs and microtwins is frequently detected within both nanocrystalline grains and ultrafine grains in the HPT AA5182 Al−Mg alloy. An example of SFs and microtwins formed within ultrafine grains is shown in Fig. 3(a). Several SFs can be seen inside a 200 nm grain of the alloy. The SF widths are in the range of 5−15 nm and the local SF density is about 2.0×10^{15} m^{-2}. The SFs and microtwins seem to be preferably located in the vicinity of GBs and sub-boundaries. Therefore, such SFs and deformation twins are believed to be formed behind

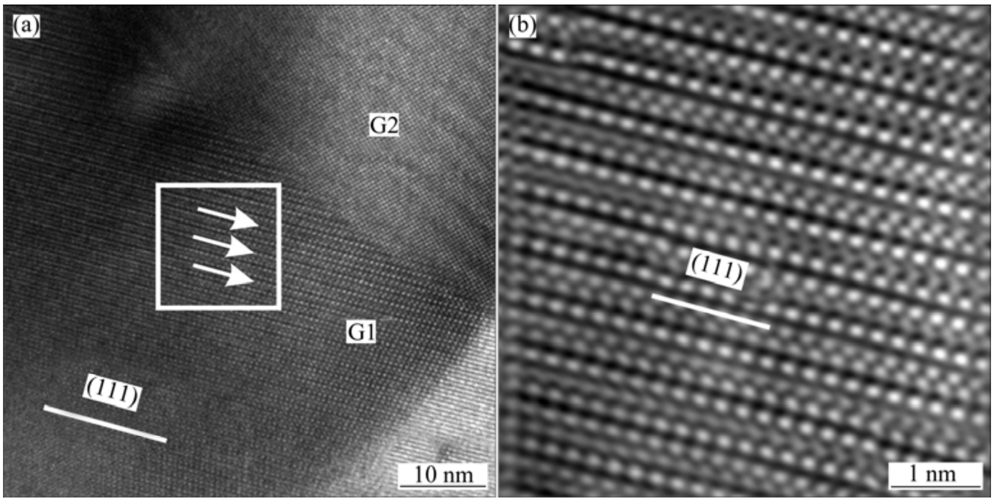

Fig. 2 HRTEM $[1\bar{1}0]$ images taken from subgrain G1 in Fig. 1(b): (a) High density of planar defects lying on (111) plane, indicated by white arrows; (b) Inverse Fourier image from white frame in Fig. 2(a), showing multiple deformation twins and SFs in subgrain

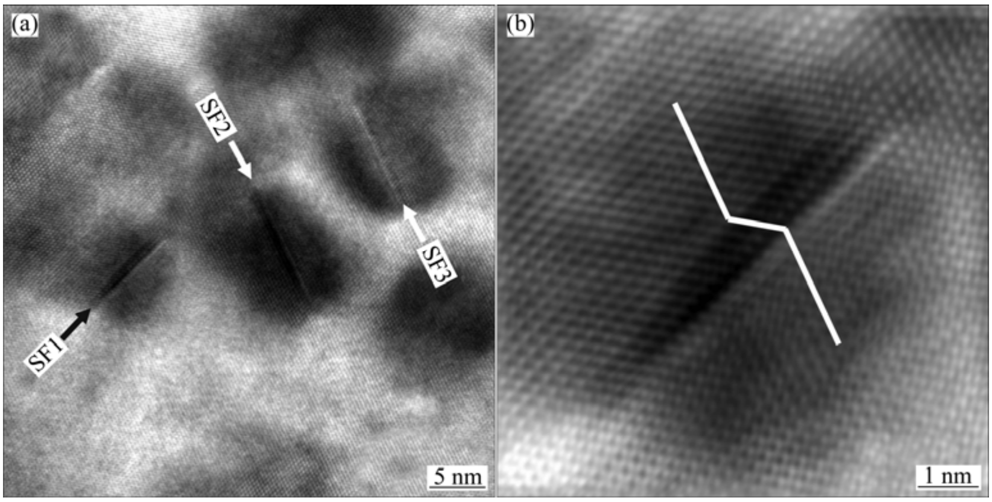

Fig. 3 HRTEM images: (a) High density of SFs in $[1\bar{1}0]$ (marked by arrows) and deformation twins within 200 nm grain in HPT AA5182 Al−Mg alloy; (b) Inverse Fourier image from SF1 in Fig. 3(a) showing deformation twin with thickness of 4 atomic planes (about 1 nm)

the moving partial dislocations which are emitted from GBs and GB junctions [10].

It has been suggested that a twin can be formed by the homogeneous mechanism involving the dynamic overlapping of SFs of dissociated dislocations in the grain interiors [10]. Deformation twins formed by such homogeneous mechanism are in fact observed by HRTEM in the HPT alloy. Figure 3(b) shows a deformation twin with thickness of 4 atomic planes (about 1 nm). Such a twin is formed by the dynamic overlapping of 4 SFs of dissociated dislocations on adjacent slip planes. The twin can grow thicker by adding more SFs on its either side.

3.3 Electron irradiation effect

Both our previous works [6,8,13] and the present observations provide experimental evidence that deformation defects including deformation twins and SFs along the {111} planes can be formed in the HPT aluminum alloys. However, BERNHARD and PETER [21] reported that radiation damage during HRTEM investigations of pure Al and Al alloys can occur. HORITA et al [20] even argued that the lattice defects along the {111} planes in Al and Al based alloys often formed (and may disappear) due to the irradiation effect during HRTEM observation.

In order to avoid confusion and artefacts and to explore the effect of electron beam radiation on the formation of the planar defects, additional HRTEM experiments similar with that by HORITA et al [20] were conducted in the HPT Al−Mg alloy. Figure 4 shows the structure change of the SFs when keeping the electron beam illumination on the same area of the ⟨110⟩ HRTEM image in Fig. 3(a) for some duration of time. As shown

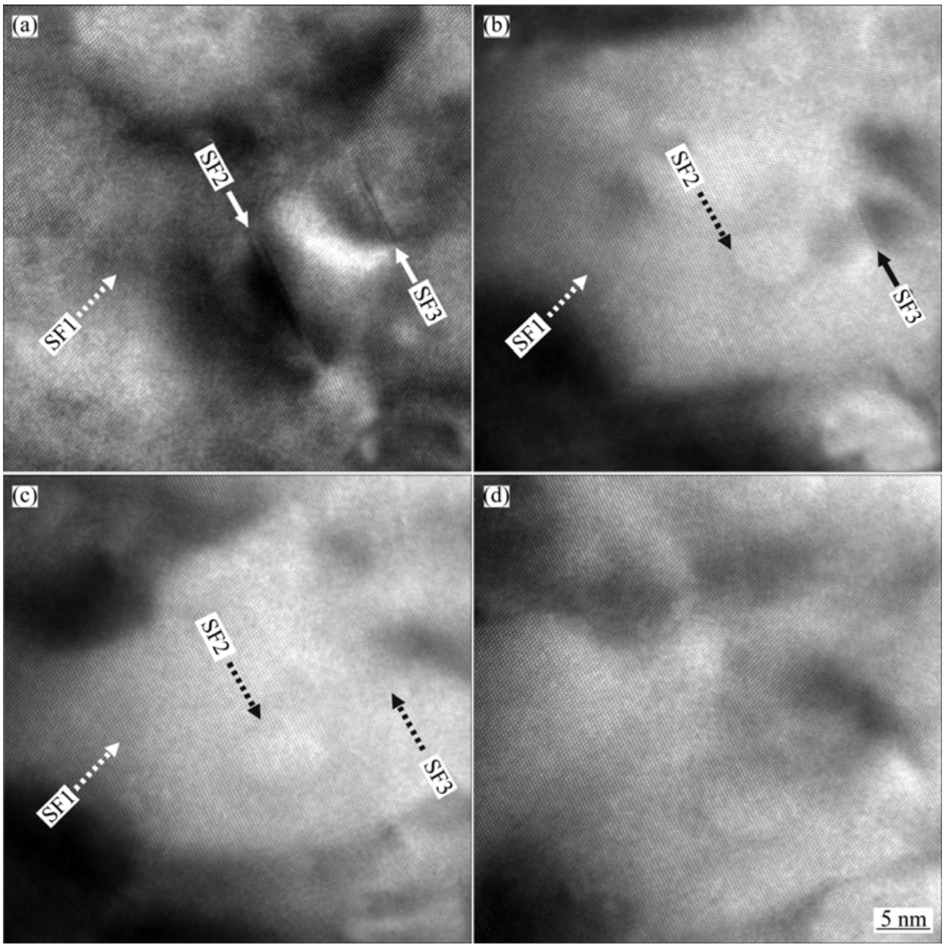

Fig. 4 HRTEM images showing disappearance of SFs as HRTEM image in Fig. 3(a) is exposed under same electron beam illumination with sequential time: (a) 4 min; (b) 17 min; (c) 21 min; (d) 28 min (Solid line arrows indicate SFs still exist as compared with image in Fig. 3(a), while dashed arrows express SFs disappear in locations where SFs appear in Fig. 3(a))

in Fig. 4, the SFs in Fig. 3(a) gradually disappear as the duration increases. When the illuminating time reaches to 4 min (Fig. 4(a)), the SF1 in Fig. 3(a) disappears while the SF2 and SF3 still exist. Note that the dashed arrows in Fig. 4 express the SFs disappear in the locations where the SFs appear in Fig. 3(a). As the beam-exposure time increases to 17 min (Fig. 4(b)), the SF2 disappears but the SF3 is distinguished. All the SFs in Fig. 3(a) disappear completely when the duration time is 21 min (Fig. 4(c)). Continuing to increase the time to 28 min, there is no any structure change in Fig. 4(d) compared to that in Fig. 4(c).

The results reveal that when a HRTEM image with high density of SFs is exposed under the electron beam for some duration of time, the SFs disappear completely. The possible reasons for this phenomenon during HRTEM observation are probably electron beam contamination or beam radiation/energy. Whether this phenomenon is due to a beam contamination or beam-energy interaction with the defects remains to be clarified. The beam contamination may be the main reason responsible for the SFs disappearance because the local quality of the HRTEM foil probably becomes bad for getting a clear image of the defects due to the contamination.

Contrary to the results of HORITA et al [20], lattice defects along the {111} planes never appear from a HRTEM image where there are originally no defects due to the beam radiation in the HPT alloy. It seems unlike that these defects will appear within a no-defect area with increasing beam-exposure time. This postulate has been actually confirmed in Fig. 4. Within 28 min of the electron illumination, only the original SFs in Fig. 3(a) disappear, no other new defects on {111} planes are observed in Figs. 4(a)−(d).

In addition, HRTEM $[1\bar{1}0]$ images in areas without any planar defects in the HPT Al−Mg alloy were chosen to further verify the postulate. An example of such HRTEM investigations is shown in Fig. 5. Figure 5(a) is the original area and no defects on {111} planes are detected in this area. Keeping the electron beam illumination on the same area in Fig. 5(a) for less

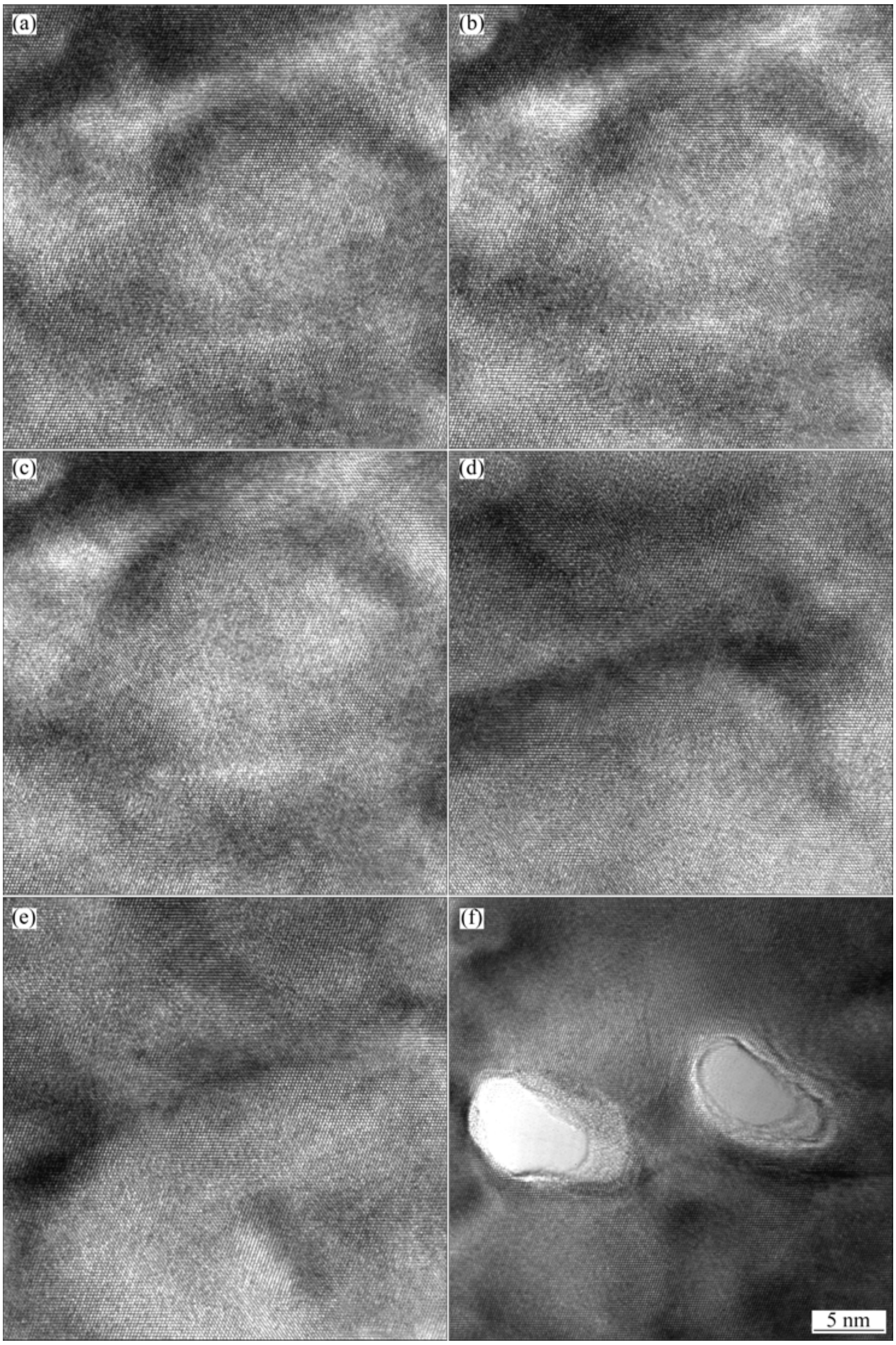

Fig. 5 Structure evolution of HRTEM $[1\bar{1}0]$ image in area without any planar defects in HPT Al−Mg alloy exposed under same electron beam illumination with sequential time: (a) 0 min; (b) 2 min; (c) 6 min; (d) 30 min; (e) 60 min; (f) 120 min

than 10 min, the structure remains unchanged (Figs. 5 (b)−(c)). As the illumination time increases to 30 min (Fig. 5(d)), the HRTEM structure has been experienced some changes but no planar defects have occurred in the area. Further increasing the time to 60 min (Fig. 5(e)), the image keeps almost the same with that in Fig. 5(d). The planar defects do not appeared even when the beam-exposure time increases to the degree that holes appear in the area (Fig. 5(f)).

Both the HRTEM examinations in Figs. 4 and 5 suggest that the planar defects observed in the SPD alloys mainly result from the significant plastic deformation and are not due to the electron radiation effect during HRTEM observation. The planar deformation defects including SFs along the {111} planes can disappear or become invisible due to electron irradiation or beam contamination but never form in the original areas without planar defects during HRTEM observation. As suggested by BERNHARD and PETER [21], the planar defects are caused by SPD and the radiation defects could be distinguished if they lie on different planes. In fact, the deformation defects of the SFs have also been confirmed by HRTEM using ⟨111⟩ beam directions in our HPT Al and Al−Mg alloys. These HRTEM ⟨111⟩ images clearly verify that the deformation defects are formed by the significant plastic deformation in the HPT alloys but these results will be published elsewhere.

It is necessary to note that our HRTEM investigations in this work only focus on the planar defects in the HPT alloy. The radiation effect on other defects such as point defects is clearly interesting but transcends the scope of the present investigation [21−28].

4 Conclusions

1) Deformation twinning, SFs and partial dislocation emissions from grain boundaries are introduced in the nanostructured Al−Mg alloys. Two twinning mechanisms predicted by MD simulations are verified. A four-layer twin formed by the dynamic overlapping of four stacking faults is observed.

2) The planar deformation defects including SFs along the {111} planes can disappear or become invisible due to electron irradiation or beam contamination but never form in the original areas without planar defects during HRTEM observation.

3) HRTEM examinations confirm that the planar defects of SFs observed in the HPT Al−Mg alloy mainly result from the significant plastic deformation and are not due to the electron radiation effect during HRTEM observation.

4) The radiation effects on other defects such as point defects and dislocations, as well as the interactions between these features in the nanostructured Al−Mg alloys are clearly interesting which need further investigations.

Acknowledgment

The authors want to acknowledge the assistance of Dr. Lilya KURMANAEVA (Forschung Center of Karlsruhe, Germany) for doing the tensile testing.

References

[1] VALIEV R Z, ZEHETBAUER M J, ESTRIN Y, HÖPPEL H W, IVANISENKO Y, HAHN H, WILDE G, ROVEN H J, SAUVAGE X, LANGDON T G. The innovation potential of bulk nanostructured materials [J]. Adv Eng Mater, 2007, 9(7): 527−533.

[2] VALIEV R Z, ISLAMGALIEV R K, ALEXANDROV I V. Bulk nanostructured materials from severe plastic deformation [J]. Prog Mater Sci, 2000, 45(2): 103−189.

[3] VALIEV R Z, ENIKEEV N A, LANGDON T G. Towards superstrength of nanostructured metals and alloys produced by SPD [J]. Kovove Mater, 2011, 49: 1−9.

[4] VALIEV R. Nanostructuring of metals by severe plastic deformation for advanced properties [J]. Nature Mater, 2004, 3(8): 511–516.

[5] ZHILYAEV A P, LANGDON T G. Using high-pressure torsion for metal processing: Fundamentals and applications [J]. Prog Mater Sci, 2008, 53(6): 893−979.

[6] LIU M P, ROVEN H J, LIU X T, UNGÁR T, BALOGH L, MURASHKIN M, VALIEV R Z. Grain refinement in nanostructured Al–Mg alloys subjected to high pressure torsion [J]. J Mater Sci, 2010, 45: 4659−4664.

[7] YAMAKOV V, WOLF D, PHILLPOT S R, GLEITER H. Dislocation-dislocation and dislocation-twin reactions in nanocrystalline Al by molecular dynamics simulation [J]. Acta Mater, 2003, 51(14): 4135−4147.

[8] LIU M P, ROVEN H J, LIU X T, MURASHKIN M, VALIEV R Z, UNGÁR T, BALOGH L. Special nanostructures in Al−Mg alloys subjected to high pressure torsion [J]. Transactions of Nonferrous Metals Society of China, 2010, 20(11): 2051−2056

[9] ZHU Y T, LIAO X Z, WU X L. Deformation twinning in bulk nanocrystalline metals: Experimental observations [J]. JOM, 2008, 60(9): 60−64.

[10] YAMAKOV V, WOLF D, PHILLPOT S R, GLEITER H. Deformation twinning in nanocrystalline Al by molecular-dynamics simulation [J]. Acta Mater, 2002, 50(20): 5005−5020.

[11] Van SWYGENHOVEN H, DERLET P M, FRØSETH A G. Stacking fault energies and slip in nanocrystalline metals [J]. Nature Mater, 2004, 3(6): 399−403.

[12] MARIAN J, KNAP J, ORTIZ M. Nanovoid cavitation by dislocation emission in aluminum [J]. Phys Rev Lett, 2004, 93(16): 165503-1−165503-4.

[13] LIU M P, ROVEN H J, MURASHKIN M, VALIEV R Z. Structural characterization by high-resolution electron microscopy of an Al−Mg alloy processed by high-pressure torsion [J]. Mater Sci Eng A, 2009, 503: 122−125.

[14] LIU M P, ROVEN H J, UNGÁR T, BALOGH L, MURASHKIN M, VALIEV R Z. Grain boundary structures and deformation defects in nanostructured Al−Mg alloys processed by high pressure torsion [J]. Mater Sci Forum, 2008, 584−586: 528−534.

[15] LIU M P, ROVEN H J, YU Y D. Deformation twins in ultrafine grained commercial aluminum [J]. Int J Mater Res, 2007, 98(3): 184−190.

[16] LIU M P, ROVEN H J, YU Y D, WERENSKIOLD J C. Deformation structures in 6082 aluminium alloy after severe plastic deformation by equal-channel angular pressing [J]. Mater Sci Eng A, 2008, 483−484: 59–63.

[17] ROVEN H J, LIU M P, MURASHKIN M, VALIEV R Z, KILMAMETOV A, UNGÁR T, BALOGH L. Nanostructures and microhardness in Al and Al−Mg alloys subjected to SPD [J]. Mater Sci Forum, 2009, 604−605: 179−185.

[18] LIU M P, ROVEN H J. High density hexagonal and rhombic shaped nanostructures in a FCC aluminum alloy induced by severe plastic deformation at room temperature [J]. Appl Phys Lett, 2007, 90(8): 083115-1−3.

[19] LIU M P, ROVEN H J, MURASHKIN M, VALIEV R Z. Deformation twins and stacking faults in an AA5182 Al−Mg alloy processed by high pressure torsion [J]. Mater Sci Forum, 2008, 579: 147−154.

[20] HORITA Z, SMITH D J, FURUKAWA M, NEMOTO M, VALIEV R Z, LANGDON T G. An investigation of grain boundaries in submicrometer-grained Al−Mg solid solution alloys using high-resolution electron microscopy [J]. J Mater Res, 1996, 97(7): 1880−1890.

[21] BERNHARD M, PETER K H. Radiation damage during HRTEM studies in pure Al and Al alloys [J]. Int J Mater Res, 2006, 97(7): 1041−1045.

[22] FURUYA K, PIAO M, ISHIKAWA N. High resolution transmission electron microscopy of defect clusters in aluminum during electron and ion irradiation at room temperature [C]//ROBERTSON I M, WAS G S, HOBBS L W. Mater Res Soc Symp Proc. Cambridge, UK: Cambridge University Press, 1997: 331−336.

[23] KIRITANI M. History, present status and future of the contribution of high-voltage electron microscopy to the study of radiation damage and defects in solids [J]. Ultramicroscopy, 1991, 39: 135−159.

[24] FARRELL K, HOUSTON J T. Suppression of radiation damage microstructure in aluminum by trace impurities [J]. J Nucl Mater, 1979, 83: 57−66.

[25] STURCKEN E F. Irradiation effects in magnesium and aluminum alloys [J]. J Nucl Mater, 1979, 82: 39−53.

[26] MAZEY D J, FRANCIS S, HUDSON J A. Observation of a partially-ordered void lattice in aluminium irradiated with 400 keV Al^+ ions [J]. J Nucl Mater, 1973, 47: 137−142.

[27] MAZEY D J, BULLOUGH R, BRAILSFORD A D. Observation and analysis of damage structure in Al and Al/Mg (N4) alloy after irradiation with 100 and 400 keV aluminium ions [J]. J Nucl Mater, 1976, 62: 73−88.

[28] MITCHELL D R G. A TEM study of radiogenic silicon precipitation in neutron irradiated aluminium [J]. Nucl Instruments and Methods Phys Res B, 1998, 140: 107−118.

大塑性变形纳米结构 Al–Mg 合金中的形变缺陷和电子辐照效应

刘满平 [1]，孙少纯 [1]，Hans J. ROVEN[2]，于瀛大 [2]，张　桢 [1]，
Maxim MURASHKIN[3], Ruslan Z. VALIEV[3]

1. 江苏大学 材料科学与工程学院，镇江 212013;
2. Department of Materials Science and Engineering, Norwegian University of Science and Technology (NTNU), NO-7491, Trondheim, Norway;
3. Institute of Physics of Advanced Materials, Ufa State Aviation Technical University, Ufa 450000, Russia

摘　要：为澄清大塑性变形纳米结构 Al−Mg 合金中形变缺陷形成的本质，采用高分辨透射电子显微镜(HRTEM)研究电子辐照对高压扭转合金中面缺陷形成的影响。结果表明：对已有高密度面缺陷的 HRTEM 图像，经电子束照射一段时间后，这些面缺陷会完全消失；而在没有缺陷的 HRTEM 图像区域进行电子辐照，即使电子束的照射提高到足以在该区域击出孔洞，整个过程均未观察到任何晶格缺陷。因此，高压扭转合金中的面缺陷主要来源于极度的塑性变形，而与 HRTEM 观察过程中的电子辐照效应无关。

关键词：Al–Mg 合金；大塑性变形；高压扭转；电子辐照；形变缺陷；透射电子显微镜

(Edited by FANG Jing-hua)